Comparative transcriptomics reveal differential gene expression in *Plasmodium vivax* geographical isolates and implications on erythrocyte invasion mechanisms

Daniel Kepple[1]*, Colby T. Ford[2,3], Jonathan Williams[1], Beka Abagero[1], Shaoyu Li[4], Jean Popovici[5], Delenasaw Yewhalaw[6,7], Eugenia Lo[1,3]*

[1] Biological Sciences, University of North Carolina, Charlotte, NC 28223, USA

[2] Bioinformatics and Genomics, University of North Carolina, Charlotte, NC 28223, USA

[3] School of Data Science, University of North Carolina, Charlotte, NC 28223, USA

[4] Mathematics and Statistics, University of North Carolina, Charlotte, NC 28223, USA

[5] Malaria Research Unit, Institut Pasteur du Cambodge, Phnom Penh, Cambodia.

[6] Tropical and Infectious Diseases Research Center, Jimma University, Jimma, Ethiopia

[7]School of Medical Laboratory Sciences, Faculty of Health Sciences, Jimma University, Jimma, Ethiopia

***Correspondence:**

Daniel Kepple (dkepple@uncc.edu); Eugenia Lo (eugenia.lo@uncc.edu)

Running title: Transcriptomic comparison of *P. vivax*

Keywords: *Plasmodium vivax*, transcriptomes, erythrocyte invasion ligands, gene expression profiles, gametocyte detection

Abstract

Plasmodium vivax uses Duffy binding protein (PvDBP1) to bind to the Duffy Antigen-Chemokine Receptor (DARC) to invade human erythrocytes. Individuals who lack DARC expression (Duffy-negative) are thought to be resistance to *P. vivax*. In recent years, *P. vivax* malaria is becoming more prevalent in Africa with a portion of these cases detected in Duffy-negatives. Apart from DBP1, members of the reticulocyte binding protein (RBP) and tryptophan-rich antigen (TRAg) families may also play a role in erythrocyte invasion. While the transcriptomes of the Southeast Asian and South American *P. vivax* are well documented, the gene expression profile of *P. vivax* in Africa and more specifically the expression level of several erythrocyte binding gene candidates as compared to DBP1 are largely unknown. This paper characterized the first *P. vivax* transcriptome in Africa and compared with those from the Southeast Asian and South American isolates. The expression of 4,404 gene transcripts belong to 12 functional groups including 43 specific erythrocyte binding gene candidates were examined. Overall, there were 10-26% differences in the gene expression profile amongst the geographical isolates, with the Ethiopian and Cambodian *P. vivax* being most similar. Majority of the gene transcripts involved in protein transportation, housekeeping, and host interaction were highly transcribed in the Ethiopian *P. vivax*. Erythrocyte binding genes including *PvRBP*2a and *PvRBP*3 expressed six-fold higher than *PvDBP*1and 60-fold higher than *PvEB*P/*DBP*2. Other genes including *PvRBP1a, PvMSP3.8*, *PvMSP3.9*, *PvTRAG2, PvTRAG14,* and *PvTRAG22* also showed relatively high expression. Differential expression was observed among geographical isolates, e.g., *PvDBP*1 and *PvEB*P/*DBP*2 were highly expressed in the Cambodian but not the Brazilian and Ethiopian isolates, whereas *PvRBP*2a and *PvRBP*2b showed higher expression in the Ethiopian and Cambodian than the Brazilian isolates. Compared to *Pvs*25, the standard

biomarker for detecting female gametocytes, *PvAP2-G* (PVP01_1440800), GAP (PVP01_1403000), and *Pvs47* (PVP01_1208000) were highly expressed across geographical samples. These findings provide an important baseline for future comparisons of *P. vivax* transcriptomes from Duffy-negative infections and highlight potential biomarkers for improved gametocyte detection.

1. Introduction

Plasmodium vivax Duffy binding protein (PvDBP1), which binds to the cysteine-rich region II of the human glycoprotein Duffy Antigen-Chemokine Receptor (DARC) (1-3), was previously thought to be the exclusive invasion mechanism for *P. vivax* (4). However, reports of *P. vivax* infections in Duffy-negative individuals (3) have raised important questions of how *P. vivax* invades erythrocytes that lack DARC expression. It was hypothesized that either mutations in *PvDBP*1 or a weakened expression of DARC allowed *P. vivax* to invade Duffy-negative erythrocytes (5, 6). Despite several mutational differences observed in *PvDBP*1 between Duffy-positive and Duffy-negative infections, these differences do not lead to binding of Duffy-negative erythrocytes (4) and suggested an alternative invasion pathway.

The *P. vivax* nuclear genome is ~29 megabases with 6,642 genes distributed amongst 14 chromosomes (7). Remarkably, across the *P. vivax* genome, approximately 77% of genes are orthologous to *P. falciparum, P. knowlesi*, and *P. yoelii* (8). Genes involved in key metabolic pathways, housekeeping functions, and membrane transporters are highly conserved between *P. vivax* and *P. falciparum* (8). However, at the genome level, *P. vivax* isolates from Africa, Southeast Asia, South America, and Pacific Oceania are significantly more polymorphic than the *P. falciparum* ones (9, 10), likely due to differences in distributional range, transmission intensity, frequency of gene flow via human movement, and host susceptibility (11).

In *P. vivax,* erythrocyte binding protein (*PvEBP*), reticulocyte binding protein (*PvRBP*), merozoite surface protein (*PvMSP*), apical membrane antigen 1 (*PvAMA1*), anchored micronemal antigen (*PvGAMA*), Rhoptry neck protein (*PvRON*), and tryptophan-rich antigen genes (*PvTRAg*) families have been suggested to play a role in erythrocyte invasion (9, 12).

*PvDBP*1, *PvMSP*1, *PvMSP*7, and *PvRBP*2c were previously shown to be highly polymorphic (13-17). *PvEBP*, a paralog of *PvDBP*1, harbors the hallmarks of a *Plasmodium* red blood cell invasion protein and is similar to *PcyM DBP*2 sequences in *P. cynomolgi* that contains a Duffy-binding like domain (18). Binding assay of *PvEBP* region II (171-484) showed moderate binding to Duffy-negative erythrocytes (4). Both *PvDBP*1 and *PvEBP* (*PvEBP/DBP*2 hereafter) exhibit high genetic diversity and are common antibody binding targets associated with clinical protection (19, 20). Several members of *PvRBP*2 (*PvRBP*2a, *PvRBP*2b, *PvRBP*2c, *PvRBP*2d, *PvRBP*2e, *PvRBP*2p1, and *PvRBP2*p2) are orthologous to *PfRh*2a, *PcyRBP*2, and *PfRh*5, with *PvRBP*2a and *PfRh*5 share high structural similarity (21, 22). *PvRBP*2b and *PvRBP*2c are orthologous to *PcyRBP*2b and *PcyRBP*2c, respectively (23). The receptor for PvRBP2a was previously identified as CD98, a type II transmembrane protein that links to one of several L-type amino acid transporters (24); the receptor for PvRBP2b is transferrin receptor 1 (TfR1) (25). The PvRBP2b-TfR1 interaction plays a critical role in reticulocyte invasion in Duffy-positive infections (25). MSP1 also shows a strong binding affinity, with high-activity binding peptides (HABPs) clustered close to fragments at positions 280–719 and 1060–1599 (26), suggesting a critical role in erythrocyte invasion. Although the *MSP*7 gene family shows no binding potential, it forms a complex with *PvTRAg*36.6 and *PvTRAg*56.2 on the surface, likely for stabilization at the merozoite surface (27). A comparison of *P. vivax* transcriptomes between *Aotus* and *Saimiri* monkeys indicated that the expression of six *PvTRAg* genes in *Saimiri P. vivax* was 37-fold higher than in the *Aotus* monkey strains (28), five of which bind to human erythrocytes (27, 29). Although most PvTRAg receptors remain poorly characterized, the receptor of PvTRAg38 has been identified as Band 3 (30).

Recent progress in transcriptomic sequencing of *P. vivax* in non-human primates has provided an overview of stage-specific gene expression profile and structure, of which thousands of splices and unannotated untranslated regions were characterized (31, 32) The transcriptomes of Cambodian (33) and Brazilian (34) *P. vivax* field isolates showed high expression levels and large populational variation amongst host-interaction transcripts. Heterogeneity of gene expression has been documented amongst *P falciparum*-infected samples, implying that the parasites can modulate the gene transcription process through epigenetic regulation (35). However, the transcriptomic profile of African *P. vivax* remains unexplored, and it is unclear if there is heterogeneity among the geographical isolates. In addition, our previous study found that two CPW-WPC genes PVP01_0904300 and PVP01_1119500 expressed in the male gametocytes, and *Pvs230* (PVP01_0415800) and *ULG*8 (PVP01_1452800) expressed in the female gametocytes were highly expressed relative to *Pvs25* in the Ethiopian *P. vivax* (36). While these genes have a potential to be used for gametocyte detection, it remains unclear if such expressional patterns are similar in other geographical isolates.

In this study, we aimed to 1) examine the overall gene expression profile of 10 Ethiopian *P. vivax* with respect to different intraerythrocytic lifecycle stages; 2) determine the expression levels of previously characterized erythrocyte binding gene candidates (9); 3) compare gene expression profiles of the Ethiopian *P. vivax* with the Cambodian (33) and Brazilian (34) isolates from *in vitro* especially for the erythrocyte binding and male/female gametocyte gene candidates. These findings provide the first description of the *P. vivax* transcriptomes in Africa. A systematic comparison of gene expression profiles among the African, Southeast Asian, and South American isolates will deepen our understanding of *P. vivax* transcriptional machinery and invasion mechanisms.

2. Materials and Methods

2.1 Ethics statement and data availability

Scientific and ethical clearance was obtained from the institutional scientific and ethical review boards of Jimma University, Ethiopia and University of North Carolina, Charlotte, USA. Written informed consent/assent for study participation was obtained from all consenting heads of households, parents/guardians (for minors under 18 years old), and individuals who were willing to participate in the study. Sequences for the 10 Ethiopian transcriptomes are available on the National Center for Biotechnology Information Short Read Archive under BioProject: PRJNA784582. All code is available on GitHub at https://github.com/colbyford/vivax_transcriptome_comparisons.

2.2 Sample preparation

Ten microscopy-confirmed *P. vivax* samples were collected from Duffy positive patients at hospitals in Jimma, Ethiopia. These patients had 4,000 parasites/µL parasitemia and had not received prior antimalarial treatment. A total of 10mL whole blood was preserved in sodium heparin tubes at the time of collection. Red blood cell pellets were isolated and cryo-preserved with two times glycerolyte 57 and stored in liquid nitrogen. Prior to culture, samples were thawed by adding 0.2V of 12% NaCl solution drop-by-drop followed by a 5-minute room temperature incubation. Ten-times volume of 1.6% NaCl solution was then added drop-by-drop to the mixture and the samples were centrifuged at 1000 rcf for 10 minutes to isolate the red blood cell pellet. This process was repeated with a 10x volume of 0.9% NaCl. Following centrifugation, the supernatant was removed via aspiration, and 18mL of sterile IMDM (also

156 containing 2.5% human AB plasma, 2.5% HEPES buffer, 2% hypoxanthine, 0.25% albumax,
157 and 0.2% gentamycin) per 1mL cryo mixture was added to each sample for a final hematocrit of
158 2%. 10% Giemsa thick microscopy slides were made to determine the majority parasite stage
159 and duration of incubation required, averaging 20-22 hours for the majority trophozoites and 40-
160 44 hours for the majority ring. Samples were incubated at 37°C in a 5% O2, 5% CO2 atmosphere
161 to allow growth to the schizont stage. *In vitro* maturation was validated through microscopic
162 smears 20-40 hours after the initial starting time, dependent on the majority stage
163 (Supplementary Figure 1A). To minimize oxidative stress, each culture was checked more than
164 two times and returned to a 5% oxygen environment immediately after checking.
165 Cultured pellets were isolated via centrifugation and placed in 10x volume trizol for RNA
166 extraction. RNA extraction was performed using direct-zol RNA prep kit according to the
167 manufacturer's protocol, followed by two rounds of DNA digestion using the DNA-free kit
168 (Zymo). Samples were analyzed with a nanodrop 2000 and RNA Qubit to ensure sample
169 concentrations were above 150 ng total for library construction. For samples with no significant
170 amount of DNA or protein contaminants, RNA libraries were constructed using Illumina rRNA
171 depletion library kits according to the manufacturer's protocol. Completed libraries were quality
172 checked using a bioanalyzer to ensure adequate cDNA was produced before sequencing. Sample
173 reads were obtained using Illumina HiSeq 2x150bp configuration to obtain at least 35 million
174 reads per sample. Sequence reads were aligned with HISAT2 (37), using the Rhisat2 R package
175 (38) to the P01 *P. vivax* reference genome and all human reads were filtered out using SAMtools
176 (39) (implemented in the R package (40)). The alignment was mapped to the P01 reference
177 annotation using the Rsubread package (41).
178

2.3 Data analyses

To further confirm samples were majority schizont stage, sequence reads of each sample were deconvoluted in CIBERSORTx (42) based on *P. berghei* homologs (43). We used the published matrix to determine the frequency of expression for each gene calculated for rings, trophozoites, and schizonts, respectively. Transcripts that were expressed 30% or more were sorted into their respective stages (Supplementary Figure 1B). All reads were annotated using the Rsubread package and classified into 12 different categories by function. We then examined the top 30 transcribed genes using the counts per million (CPM) metric.

Our previously published whole genome sequence data identified several mutations and structural polymorphisms in genes from the *PvEBP*, *PvRBP*, *PvMSP*, and *PvTRAg* gene families that are likely to involve in erythrocyte invasion (9). Specific binding regions in some of the genes such as *PvDBP*1, *PvEBP/DBP2*, *PvRBP*2b, and *PvMSP*3 have been identified (44). To further explore the putative function, we compared relative expression levels of 43 erythrocyte binding gene candidates (Supplementary Table 1) in the 10 Ethiopian *P. vivax* samples with other geographical isolates that were of majority schizont stage. We used the CPM and TPM (transcripts per million) metrics in R package edgeR (45). The CPM metric was used to obtain the top 30 transcripts overall and does not consider gene length, while TPM considers gene length for normalization and allows an unbiased conclusion to be made relative between and to other transcriptomes (34). We then transformed the data using *log*(2)TPM+1 to illustrate relative expression levels via a heat map with an average abundance. We also selected 25 gametocyte gene candidates, 15 of which were shown to correlate to female gametocyte development and nine to male gametocytes (36, 46), to assess their expression levels relative to the standard

*Pvs*25 in the samples. In addition, we examined the expression of AP2-G that is a critical transcription factor for both male and female gametocyte development (47).

2.4 Comparison of datasets

RNA-seq data of four *in vitro* Cambodian (33) and two *in vitro* Brazilian (34) *P. vivax* samples were downloaded from the GitHub repository and analyzed with the same bioinformatic methods described above to minimize potential batch effects. Samples were deconvoluted using the same matrix. The Ethiopian *P. vivax* samples were cultured and sequenced using similar protocol as the Cambodian (33) and Brazilian (34) ones with slight modifications in media and library preparation. We obtained the average expression and standard deviation in TPM for each gene target and determined potential difference in transcription levels by conducting pairwise differential expression (DE) analysis among the Cambodian, Brazilian, and Ethiopian samples. The expression level of 6,829 genes were examined for DE by edgeR dream (45, 48) and variancePartition (49), with adjusted p-value<1.0e-6 for DE gene concordance. A linear mixed effects models was used to ensure accuracy in triplicated Brazilian samples, and the Kenward-Roger method was used to estimate the effective degree of freedom for hypothesis testing due to small sample sizes.

3. Results

3.1 Overview of the Ethiopian *P. vivax* transcriptomes

All 10 Ethiopian *P. vivax* samples originated from Duffy-positive patients. Based on deconvolution, all 10 Ethiopian *P. vivax* samples had similar proportions of trophozoite and schizont stage (Figure 1A). Only less than 1% of the sequence reads belong to the ring stage.

Microscopic results corroborated the deconvolution analyses showing similar proportion of parasite stages in a subset of samples (Figure 1B). The deconvolution of *P. vivax* sequence reads from the Cambodian and Brazilian samples also showed no significant difference in the proportions of trophozoites or schizonts (P>0.05; Figure 1A).

Overall, about 64% (4,404 out of 6,830) of the genes were detected with transcription in the Ethiopian *P. vivax* (Supplementary Table 2). Of the 4,404 genes, 69% (2,997) were annotated with known functions and 31% (1,407 genes) remain uncharacterized (Figure 2A). We normalized each sample expression profile to TPM to remove technical bias in the sequences and ensure gene expressions were directly comparable within and between samples (Supplementary Table 2). Of the 2,997 genes with known function, 21.7% are responsible for housekeeping, and 14.2% genes for post-translation modifications (PTMs) and regulation. The PIR proteins account for 4.8% (212) of all the identified genes and ~2.8% of the genes are involved in host-pathogen interactions. Nearly 52% of all detectable transcripts (2,288 genes) were expressed at a threshold of 20 TPM or above, which were considered as highly transcribed (Figure 2B). These highly transcribed transcripts showed similar proportions of gene categories including unknown, PTM/regulatory, DNA regulation, replication/elongation, host interactions, cell signaling, and resistance. Only transcripts involved in transport and housekeeping showed a slight increase of 2.9% and 1.48%, respectively, indicating a higher activity relative to the other categories. By contrast, transcripts involved in RNA regulation, PIR, and ribosomal activity showed a slight decrease of 2.19%, 1.79%, and 1.71%, indicating an overall lower activity compared to other categories (Figure 2B).

3.2 Top 30 highly expressed transcripts of Ethiopian *P. vivax*

For the 10 Ethiopian *P. vivax* transcriptomes, four genes including PVP01_1000200 (PIR protein), PVP01_0202900 (18s rRNA), PVP01_0319600 (RNA-binding protein), and PVP01_0319500 (unknown function) were the most highly expressed among the others (Figure 3). Transcripts involved in housekeeping and PTM regulation each account for 23.3% of the top 30 highly expressed genes. Among genes involved in host-interactions, PVP01_0715400 (merozoite organizing protein), PVP01_0816800 (protein RIPR), PVP01_1402400 (reticulocyte binding protein 2a), and PVP01_1469400 (reticulocyte binding protein 3) are highly expressed. Five gene transcripts including PVP01_1000200 from the PIR family, PVP01_0319500 of unknown function, PVP01_0202900 a 18S rRNA, PVP01_1329600 a putative glutathione S-transferase, and PVP01_0418800 a putative pentafunctional AROM polypeptide showed most variable expression levels among the 10 samples, with a standard deviation of 20,000 and higher CPM (Figure 3). Three other genes including PVP01_0202700 (28S ribosomal RNA), PVP01_1137600 (basal complex transmembrane protein 1), PVP01_1243600 (replication factor C subunit 3) showed moderate variation ranging from 1,397 to 1,033 CPM. All other genes such as PVP01_1206500 (elongation factor Tu) and PVP01_1011500 (an unclassified protein) showed consistent expression level with variation under 1,000 CPM among samples (Figure 3).

3.3 Differentially expressed genes among geographical *P. vivax*

The overall gene expression profile was similar between the Ethiopian and Cambodian *P. vivax*, but different from the Brazilian ones (Figure 4A; Supplementary Table 3). Several genes involved in DNA regulation, host-interactions, replication, ribosomal, and transportation were upregulated in the Ethiopian and Cambodian isolates but showed considerable downregulation in Brazilian ones. Based on the Kenward-Roger DE analyses, a total of 1,831 differentially

expressed genes were detected between the Cambodian and Brazilian isolates (CvB), 1,716 between the Ethiopian and Brazilian (EvB), and 721 between the Ethiopian and Cambodian (EvC) isolates (Figure 4B-D). The EvC analysis showed the lowest differentiation with only 10.6% of the entire transcriptome (Figure 4B), while EvB and CvB showed a greater differentiation of 25.1% and 26.8%, respectively (Figures 4C & D). For the 721 genes that were differentially expressed between the Cambodian and Ethiopian *P. vivax*, nearly half of them were significantly upregulated in Ethiopia compared to Cambodia (Figure 4B). Four genes including PVP01_0208700 (V-type proton ATPase subunit C), PVP01_0102800 (chitinase), PVP01_0404000 (PIR protein), and PVP01_0808300 (zinc finger (CCCH type protein) showed low levels of transcription ($\log_{10}$*P*-value>50; Figure 4B) compared to other DE genes. By contrast, two genes including PVP01_1329600 (glutathione S-transferase) and PVP01_MIT03400 (cytochrome b) were highly transcribed ($\log_2$fold change>10). For the 1,716 genes that were differentially expressed between the Ethiopian and Brazilian *P. vivax*, 914 of them were highly transcribed (Figure 3C). Of these, three genes including PVP01_1412800 (M1-family alanyl aminopeptidase), PVP01_0723900 (protein phosphatase-beta), and PVP01_0504500 (28S ribosomal RNA) showed a $\log_{10}$*P*-value greater then 75, indicating substantial expressional differences. For the 1,831 genes that were differentially expressed between the Cambodian and Brazilian *P. vivax*, 948 of them were highly transcribed (Figure 4D). Four genes including PVP01_1005900 (ATP-dependent RNA helicase DDX41), PVP01_0318700 (tRNAHis guanylyltransferase), PVP01_1334600 (60S ribosomal protein L10), and PVP01_1125300 (SURP domain-containing protein) showed substantial expressional differences with $\log_{10}$*P*-value greater than 75. Two genes, PVP01_0010550 (28S ribosomal RNA) and PVP01_0422600 (early transcribed membrane protein), were shown with low

293 expression (log_{10}fold change<-12), while one gene PVP01_0901000 (PIR protein) with
294 substantial expression (log_{10}fold change>12). These comparisons further demonstrated the
295 differences in transcriptional patterns between geographical isolates.
296

297 ## 3.4 Expression of genes related to erythrocyte invasion

298 Of the 43 candidate genes associated with erythrocyte binding function, *PvDBP*1 on average
299 showed about 10-fold higher expression than *PvEBP/DBP*2, which showed very low expression
300 in four of the Ethiopian *P. vivax* samples (Figure 5). *PvRBP2*b showed four-fold higher
301 expression than *PvEBP/DBP*2, but 50% less than *PvDBP*1. *PvRBP*2a showed consistently the
302 highest expression across all samples, with about 6-fold, 67-fold, and 15-fold higher expression
303 than *PvDBP*1, *PvEBP/DBP*2, and *PvRBP2*b, respectively. Other genes including *PvMSP*3.8,
304 *PvTRAg*14, and *PvTRAg*22 also showed higher expression than *PvDBP*1. Of the 15 *PvTRAg*
305 genes, only *PvTRAg*14 and *PvTRAg*22 showed expression higher than *PvDBP*1; *PvTRAg*23 and
306 *PvTRAg*24 showed the lowest expression. Other putatively functional ligands including *PvRA*
307 and *PvRON4* showed 7-10 times lower expression compared to *PvDBP*1, though *PvGAMA*,
308 *PvRhopH*3, *PvAMA*1, and *PvRON*2 were expressed higher than *PvEBP/DBP*2.
309 We further compared the expressional pattern of these 43 genes in the Ethiopian *P. vivax*
310 with the Cambodian and Brazilian isolates (Figure 6). Members of the *PvDBP* and *PvRBP* gene
311 family showed generally higher expression in the Cambodian *P. vivax* than the other isolates
312 (Figure 6A). For instance, the expression of *PvDBP*1, *PvRBP*1a, and *PvRBP*1b were
313 significantly higher in the Cambodian than the other isolates (P<0.01), whereas *PvRBP*2a and
314 *PvRBP*2b showed higher expression in the Ethiopian *P. vivax* than the others. Compared to the
315 *PvDBP* and *PvRBP* gene families, the expression patterns of *PvMSP* were different (Figure 6B).

316 Most of the *MSP* gene members including *PvMSP*3.5*, PvMSP*3.11*,* and *PvMSP*4 showed
317 substantially higher expression in the Brazilian *P. vivax* than the other isolates (P<0.01). Only
318 *PvMSP*3.8 of the 12 *PvMSP* genes was expressed significantly higher in the Ethiopian than the
319 others (P<0.01; Figure 6B). Of the 16 *PvTRAg* genes, *PvTRAg*14 and *PvTRAg*22 showed
320 significantly higher expression in the Ethiopian isolates compared to the others (P<0.05; Figure
321 6C). Eight other members including *PvTRAg*2b, *PvTRAg*7, *PvTRAg*19, *PvTRAg*20, *PvTRAg*21,
322 *PvTRAg*23, *PvTRAg*24, and *PvTRAg*38 showed significantly higher expression in the Brazilian
323 isolates than the others (P<0.05; Figure 6C). The remaining nine putatively functional ligands
324 showed relatively similar expression levels, except for *PvMA*, *PvRhopH3,* and *PvTrx-mero* that
325 were highly expressed in the Brazilian isolates (P<0.05; Figure 6D).
326

327 ## 3.5 Expression of female and male gametocyte genes

328 Based on the expression level of *Pvs25* (PvP01_0616100), all 10 Ethiopian *P. vivax* samples
329 contained submicroscopic gametocytes, in addition to the four samples from Cambodia and two
330 samples from Brazil (Figure 7). Amongst the 26 gametocyte-related genes, *PvAP2-G*
331 (PVP01_1440800) as well as the gametocyte associated protein, GAP (PVP01_1403000) and
332 *Pvs47* (PVP01_1208000) from female and male gametocytes, respectively, showed the highest
333 expression across the Ethiopian, Cambodian, and Brazilian isolates, and were consistently higher
334 than *Pvs*25 (Figure 7). This expression pattern suggests the potential utility of these three genes
335 as better gametocyte biomarkers across geographical isolates. Other genes indicated differential
336 expression patterns among isolates, e.g., the female gametocyte gene PVP01_0904300 (CPW-
337 WPC family protein) showed consistently high levels of expression in both the Ethiopian and
338 Cambodian isolates, though much lower in the Brazilian ones. On the other hand,

339 PVP01_1302200 (high mobility group protein B1) and PVP01_1262200 (fructose 1,6-
340 bisphosphate aldolase) from the female and male gametocytes showed the highest expression
341 levels in Brazilian *P. vivax* but not the Ethiopian and Cambodian ones.
342

343 # 4. Discussion

344 This study is the first to examine the transcriptomic profile of *P. vivax* from Africa and compare
345 gene expression among geographical isolates. Approximately 32% of the detected transcripts are
346 of unknown function, some of which such as PVP01_0319500, PVP01_1011500, and
347 PVP01_1228800 were among the highest expressed and could play critical function. It is not
348 surprising that 23% of the highly expressed transcripts belong to housekeeping function, such as
349 several zinc fingers and ATP-synthase proteins. Besides, there is a large number of highly
350 expressed protein regulators and PTMs that have not been thoroughly examined. For example,
351 PVP01_1444000, a ubiquitin-activating enzyme, was among the highest expressed transcripts
352 but with unclear function. Several other protein kinases, lysophospholipases, and chaperones
353 were also highly expressed but their role in intercellular signaling pathways is unclear. It is worth
354 noting that a great proportion of transcripts responsible for ribosomal protein production were
355 also highly expressed. These ribosomal proteins support intraerythrocytic development of the
356 parasites from one stage to another.

357 Members of the RBP family including *PvRBP1a*, *PvRBP2a*, *PvRBP2b*, and *PvRBP3*
358 were consistently highly expressed across the Ethiopian and Cambodian but not the Brazilian
359 isolates, suggestive of potential differences in their role of erythrocyte invasion. Recent studies
360 showed that the binding regions of *PvRBP1a* and *PvRBP1b* are homologous to that of *PfRh*4,
361 and the amino acids at site ~339-599 were confirmed to interact with human reticulocytes (50).

Though the host receptors of both PvRBP1a and PvRBP1b proteins are unclear, their receptors are neuraminidase resistant (22). The PvRBP2b-TfR1 interaction plays a critical role in reticulocyte invasion in Duffy-positive infections (25). *PvRBP*2d, *PvRBP*2e, and *PvRBP*3 are pseudogenes that share homology with other *PvRBP*s but encode for nonfunctional proteins (51). The extent to which of these *PvRBP* genes involve, if any, in erythrocyte invasion remains unclear and requires functional assays in broad samples. The high expression of *PvRBP* genes in Ethiopia could be related to a greater proportion of individuals with weak DARC expression (i.e., Duffy-negatives) (3); whereas in Cambodia and the inland regions of Brazil, populations are predominantly Duffy-positive (3). Given that *P. falciparum* can modulate gene expression in response to their hosts through epigenetic regulation (35, 52, 53), higher *PvRBP* expression in the Ethiopian *P. vivax* may allow the parasites to infect and adapt to both Duffy-positive and Duffy-negative populations (54). Further investigation on the expression and binding affinity of these *PvRBP* genes in different Duffy groups is necessary.

Another invasion protein, RIPR, was also among the highly expressed transcripts in *P. vivax*. RIPR is currently known as a vaccine target in *P. falciparum* (55), where RIPR (PfRH5) binds to the erythrocyte receptor basigin (56, 57). The PfRh5 complex is composed of PfRh5, Ripr, CyRPA, and Pf113, which collectively promote successful merozoite invasion of erythrocytes by binding to basigin (BSG, CD147) (57, 58). A BSG variant on erythrocytes, known as Ok^{a-}, has been shown to reduce merozoite binding affinities and invasion efficiencies (56), though this has only been reported in individuals of Japanese ancestry (59). Despite the clear role of RIPR in *P. falciparum*, *P. vivax* RIPR does not seem to bind to BSG (60) and the exact role of RIPR and its binding target(s) remains unclear.

The KR-DE analysis showed 10-26% variation among the transcriptomes of the three countries, with the Ethiopian and Cambodian *P. vivax* being most similar whereas the Cambodian and Brazilian *P. vivax* most different. Genes that showed the highest levels of differentiation were those involved in housekeeping, PIR, and ribosomal functions. The exact reason for such differences amongst the geographical *P. vivax* isolates remains unclear. Previous whole genome sequencing analyses indicated that the Ethiopian, Cambodian, and Brazilian *P. vivax* are independent subpopulations, with isolates from Southeast Asia and East Africa share the most common ancestry (61). This genetic relationship may explain variations in the expression profiles. The high expression observed for some PIR proteins, such as PVP01_1000200, in the Cambodian and Ethiopian *P vivax* may suggest the prominent role of VIR antigens in epigenetic regulation associated with host exposure and immune responses (35, 52, 53), and such immune responses could vary in diverse geographical settings (62-64). Varying expression of ribosomal proteins, such as PVP01_0827400 (60S ribosomal protein L26) and PVP01_1013900 (40S ribosomal protein S9, putative) may be attributed to host nutrition, which is directly proportional to the speed of replication in *P. berghei* (65). In *P. falciparum*, host nutrition has been shown to significantly alter gene expression related to housekeeping, metabolism, replication, and invasion/transmission (65). Malnourishment has a protective effect to *P. vivax* infections in people from the western Brazilian Amazon (66). In zebra fish, sex determination can cause significant expressional differences in the housekeeping genes (67), suggesting that sexual development factors may alter expression profiles. The marked differences observed in the Brazilian isolates may also be attributed to the presence of ring stage parasites or oxidative stress related to different *in vitro* environments. Future studies should

406 expand geographical samples of *P. vivax* and examine further host factors associated with gene
407 expression.

408 In this study, the deconvolution of stage-specific transcripts was based on the *P. berghei*
409 orthologues rather than the single-cell RNA-seq data of *P. vivax* because the latter showed little
410 expression from the ring stage. To date, *P. berghei* remains the most comprehensively
411 characterized single-cell data for both sexual and asexual blood stages of *Plasmodium* (68, 69),
412 and their orthologues have been shown to be reliable for determining stage-specific transcripts
413 (46). In primates, most *P vivax* genes have been shown to transcribe during a short period in the
414 intraerythrocytic cycle (31) with a high proportion of late-schizont transcripts expressed as early
415 as the trophozoite stage. In *P. berghei*, the process of gametocyte development and genes involve
416 in sequestration are transcribed much earlier during the trophozoite-schizont transition stage.
417 Male gametocyte development precursors are expressed in the asexual stages prior to the onset of
418 gametocyte development (70, 71). For example, the transcription factor *AP2-G* in *P. vivax*
419 expresses early in the asexual stage for parasites that are committed to sexual development (47).
420 These factors hinder deconvolution efforts, making it challenging to identify precisely which
421 genes are transcribed in each stage. Future studies should consider combining *in vivo* (rich in
422 ring and trophozoites) and *in vitro* (rich in trophozoites and schizonts) RNA-seq data to provide
423 a more comprehensive and reliable stage-specific model for deconvolution.

424 Low density *P. vivax* gametocytes in asymptomatic carriers can significantly contribute
425 to transmission (72, 73). In areas with low transmission, submicroscopic infections are hidden
426 reservoirs for parasites with high proportions of infectious gametocytes (74). The current
427 gametocyte biomarkers *Pvs25* (PVP01_0616100) and *Pvs16* (PVP01_0305600) account only for
428 female gametocytes (75), and grossly underestimate the total gametocyte densities. We

previously described two alternative female (PVP01_0415800 and PVP01_0904300) and one male (PVP01_1119500) gametocyte genes that show higher expression than *Pvs*25 in the Ethiopian isolates (36). Nevertheless, these genes showed relatively low expression in the Cambodian and Brazilian isolates. By contrast, *PvAP2-G* (PVP01_1440800), GAP (PVP01_1403000), and *Pvs47* (PVP01_1208000) were moderately expressed across all geographical isolates and at a level higher than *Pvs25*. These genes warrant further investigations on their potential utility as gametocyte biomarkers in low-density infections, as well as their exact role in gametocyte development.

5. Conclusion

This paper characterized the first *P. vivax* transcriptome from Africa and identified several host-interaction gene transcripts, including *PvRBP2*a, *PvMSP*3.8, *PvTRAg*14, and *PvTRAg*22 that were highly expressed compared to *PvDBP*1 in Duffy-positive individuals. These transcripts may play prominent roles in erythrocyte invasion and merit further investigations on their binding affinity and function. We further demonstrated 10-26% differences in the gene expression profile amongst the geographical isolates, with the Ethiopian and Cambodian *P. vivax* being most similar. These findings provide an important baseline for future comparisons of *P. vivax* transcriptomes from Duffy-negative infections. Furthermore, *PvAP2-G* (PVP01_1440800), GAP (PVP01_1403000), and *Pvs47* (PVP01_1208000) of both female and male gametocytes showed higher expression than the standard *Pvs25* in all geographical *P. vivax*. These gene may provide better gametocyte detection for low-density infections.

Acknowledgements. We thank the field team from Jimma University for their technical assistance; the communities and hospitals for their support and willingness to participate in this research; and undergraduate students at UNC Charlotte for assistance with the experiments.

Financial support. This research was funded by National Institutes of Health R01AI162947.

Potential conflicts of interest. The authors declare no conflict of interest.

References

1. Chitnis CE, Miller LH. Identification of the erythrocyte binding domains of Plasmodium vivax and Plasmodium knowlesi proteins involved in erythrocyte invasion. J Exp Med. 1994;180(2):497-506.
2. Fang XD, Kaslow DC, Adams JH, Miller LH. Cloning of the Plasmodium vivax Duffy receptor. Mol Biochem Parasitol. 1991;44(1):125-32.
3. Howes RE, Patil AP, Piel FB, Nyangiri OA, Kabaria CW, Gething PW, et al. The global distribution of the Duffy blood group. Nat Commun. 2011;2:266.

4. Gunalan K, Lo E, Hostetler JB, Yewhalaw D, Mu J, Neafsey DE, et al. Role of Plasmodium vivax Duffy-binding protein 1 in invasion of Duffy-null Africans. Proc Natl Acad Sci U S A. 2016;113(22):6271-6.
5. Menard D, Barnadas C, Bouchier C, Henry-Halldin C, Gray LR, Ratsimbasoa A, et al. Plasmodium vivax clinical malaria is commonly observed in Duffy-negative Malagasy people. Proc Natl Acad Sci U S A. 2010;107(13):5967-71.
6. Menard D, Chan ER, Benedet C, Ratsimbasoa A, Kim S, Chim P, et al. Whole genome sequencing of field isolates reveals a common duplication of the Duffy binding protein gene in Malagasy Plasmodium vivax strains. PLoS Negl Trop Dis. 2013;7(11):e2489.
7. Auburn S, Bohme U, Steinbiss S, Trimarsanto H, Hostetler J, Sanders M, et al. A new Plasmodium vivax reference sequence with improved assembly of the subtelomeres reveals an abundance of pir genes. Wellcome Open Res. 2016;1:4.
8. Carlton JM, Adams JH, Silva JC, Bidwell SL, Lorenzi H, Caler E, et al. Comparative genomics of the neglected human malaria parasite Plasmodium vivax. Nature. 2008;455(7214):757-63.
9. Ford A, Kepple D, Abagero BR, Connors J, Pearson R, Auburn S, et al. Whole genome sequencing of Plasmodium vivax isolates reveals frequent sequence and structural polymorphisms in erythrocyte binding genes. PLoS Negl Trop Dis. 2020;14(10):e0008234.
10. White MT, Shirreff G, Karl S, Ghani AC, Mueller I. Variation in relapse frequency and the transmission potential of Plasmodium vivax malaria. Proc Biol Sci. 2016;283(1827):20160048.
11. Auburn S, Benavente ED, Miotto O, Pearson RD, Amato R, Grigg MJ, et al. Genomic analysis of a pre-elimination Malaysian Plasmodium vivax population reveals selective pressures and changing transmission dynamics. Nat Commun. 2018;9(1):2585.
12. Roesch C, Popovici J, Bin S, Run V, Kim S, Ramboarina S, et al. Genetic diversity in two Plasmodium vivax protein ligands for reticulocyte invasion. PLoS Negl Trop Dis. 2018;12(10):e0006555.
13. Chen SB, Wang Y, Kassegne K, Xu B, Shen HM, Chen JH. Whole-genome sequencing of a Plasmodium vivax clinical isolate exhibits geographical characteristics and high genetic variation in China-Myanmar border area. BMC Genomics. 2017;18(1):131.
14. Cornejo OE, Fisher D, Escalante AA. Genome-wide patterns of genetic polymorphism and signatures of selection in Plasmodium vivax. Genome Biol Evol. 2014;7(1):106-19.
15. Diez Benavente E, Ward Z, Chan W, Mohareb FR, Sutherland CJ, Roper C, et al. Genomic variation in Plasmodium vivax malaria reveals regions under selective pressure. PLoS One. 2017;12(5):e0177134.
16. Pearson RD, Amato R, Auburn S, Miotto O, Almagro-Garcia J, Amaratunga C, et al. Genomic analysis of local variation and recent evolution in Plasmodium vivax. Nat Genet. 2016;48(8):959-64.
17. Rice BL, Acosta MM, Pacheco MA, Carlton JM, Barnwell JW, Escalante AA. The origin and diversification of the merozoite surface protein 3 (msp3) multi-gene family in Plasmodium vivax and related parasites. Mol Phylogenet Evol. 2014;78:172-84.
18. Hester J, Chan ER, Menard D, Mercereau-Puijalon O, Barnwell J, Zimmerman PA, et al. De novo assembly of a field isolate genome reveals novel Plasmodium vivax erythrocyte invasion genes. PLoS Negl Trop Dis. 2013;7(12):e2569.

19. Carias LL, Dechavanne S, Nicolete VC, Sreng S, Suon S, Amaratunga C, et al. Identification and Characterization of Functional Human Monoclonal Antibodies to Plasmodium vivax Duffy-Binding Protein. J Immunol. 2019;202(9):2648-60.
20. He WQ, Shakri AR, Bhardwaj R, Franca CT, Stanisic DI, Healer J, et al. Antibody responses to Plasmodium vivax Duffy binding and Erythrocyte binding proteins predict risk of infection and are associated with protection from clinical Malaria. PLoS Negl Trop Dis. 2019;13(2):e0006987.
21. Gruszczyk J, Lim NT, Arnott A, He WQ, Nguitragool W, Roobsoong W, et al. Structurally conserved erythrocyte-binding domain in Plasmodium provides a versatile scaffold for alternate receptor engagement. Proc Natl Acad Sci U S A. 2016;113(2):E191-200.
22. Han JH, Lee SK, Wang B, Muh F, Nyunt MH, Na S, et al. Identification of a reticulocyte-specific binding domain of Plasmodium vivax reticulocyte-binding protein 1 that is homologous to the PfRh4 erythrocyte-binding domain. Sci Rep. 2016;6:26993.
23. Tachibana S, Sullivan SA, Kawai S, Nakamura S, Kim HR, Goto N, et al. Plasmodium cynomolgi genome sequences provide insight into Plasmodium vivax and the monkey malaria clade. Nat Genet. 2012;44(9):1051-5.
24. Malleret B, El Sahili A, Tay MZ, Carissimo G, Ong ASM, Novera W, et al. Plasmodium vivax binds host CD98hc (SLC3A2) to enter immature red blood cells. Nat Microbiol. 2021;6(8):991-9.
25. Gruszczyk J, Kanjee U, Chan LJ, Menant S, Malleret B, Lim NTY, et al. Transferrin receptor 1 is a reticulocyte-specific receptor for Plasmodium vivax. Science. 2018;359(6371):48-55.
26. Rodriguez LE, Urquiza M, Ocampo M, Curtidor H, Suarez J, Garcia J, et al. Plasmodium vivax MSP-1 peptides have high specific binding activity to human reticulocytes. Vaccine. 2002;20(9-10):1331-9.
27. Tyagi K, Hossain ME, Thakur V, Aggarwal P, Malhotra P, Mohmmed A, et al. Plasmodium vivax Tryptophan Rich Antigen PvTRAg36.6 Interacts with PvETRAMP and PvTRAg56.6 Interacts with PvMSP7 during Erythrocytic Stages of the Parasite. PLoS One. 2016;11(3):e0151065.
28. Gunalan K, Sa JM, Moraes Barros RR, Anzick SL, Caleon RL, Mershon JP, et al. Transcriptome profiling of Plasmodium vivax in Saimiri monkeys identifies potential ligands for invasion. Proc Natl Acad Sci U S A. 2019;116(14):7053-61.
29. Tyagi RK, Sharma YD. Erythrocyte Binding Activity Displayed by a Selective Group of Plasmodium vivax Tryptophan Rich Antigens Is Inhibited by Patients' Antibodies. PLoS One. 2012;7(12):e50754.
30. Alam MS, Choudhary V, Zeeshan M, Tyagi RK, Rathore S, Sharma YD. Interaction of Plasmodium vivax Tryptophan-rich Antigen PvTRAg38 with Band 3 on Human Erythrocyte Surface Facilitates Parasite Growth. J Biol Chem. 2015;290(33):20257-72.
31. Sa JM, Cannon MV, Caleon RL, Wellems TE, Serre D. Single-cell transcription analysis of Plasmodium vivax blood-stage parasites identifies stage- and species-specific profiles of expression. PLoS Biol. 2020;18(5):e3000711.
32. Zhu L, Mok S, Imwong M, Jaidee A, Russell B, Nosten F, et al. New insights into the Plasmodium vivax transcriptome using RNA-Seq. Sci Rep. 2016;6:20498.
33. Siegel SV, Chappell L, Hostetler JB, Amaratunga C, Suon S, Bohme U, et al. Analysis of Plasmodium vivax schizont transcriptomes from field isolates reveals heterogeneity of expression of genes involved in host-parasite interactions. Sci Rep. 2020;10(1):16667.

34. Rangel GW, Clark MA, Kanjee U, Goldberg JM, MacInnis B, Jose Menezes M, et al. Plasmodium vivax transcriptional profiling of low input cryopreserved isolates through the intraerythrocytic development cycle. PLoS Negl Trop Dis. 2020;14(3):e0008104.
35. Cortes A, Crowley VM, Vaquero A, Voss TS. A view on the role of epigenetics in the biology of malaria parasites. PLoS Pathog. 2012;8(12):e1002943.
36. Ford A, Kepple D, Williams J, Kolesar G, Ford CT, Abebe A, et al. Gene Polymorphisms Among Plasmodium vivax Geographical Isolates and the Potential as New Biomarkers for Gametocyte Detection. Front Cell Infect Microbiol. 2021;11:789417.
37. Kim D, Paggi JM, Park C, Bennett C, Salzberg SL. Graph-based genome alignment and genotyping with HISAT2 and HISAT-genotype. Nat Biotechnol. 2019;37(8):907-15.
38. Soneson C. hisat2: R Wrapper for HISAT2 Aligner. R package version 1120,. 2022.
39. Li H, Handsaker B, Wysoker A, Fennell T, Ruan J, Homer N, et al. The Sequence Alignment/Map format and SAMtools. Bioinformatics. 2009;25(16):2078-9.
40. Morgan M PH, Obenchain V, Hayden N. Rsamtools: Binary alignment (BAM), FASTA, variant call (BCF), and tabix file import. R package version 2120. 2022.
41. Liao Y, Smyth GK, Shi W. The R package Rsubread is easier, faster, cheaper and better for alignment and quantification of RNA sequencing reads. Nucleic Acids Res. 2019;47(8):e47.
42. Newman AM, Steen CB, Liu CL, Gentles AJ, Chaudhuri AA, Scherer F, et al. Determining cell type abundance and expression from bulk tissues with digital cytometry. Nat Biotechnol. 2019;37(7):773-82.
43. Tebben K, Dia A, Serre D. Determination of the Stage Composition of Plasmodium Infections from Bulk Gene Expression Data. mSystems. 2022:e0025822.
44. Kepple D, Pestana K, Tomida J, Abebe A, Golassa L, Lo E. Alternative Invasion Mechanisms and Host Immune Response to Plasmodium vivax Malaria: Trends and Future Directions. Microorganisms. 2020;9(1).
45. Robinson MD, McCarthy DJ, Smyth GK. edgeR: a Bioconductor package for differential expression analysis of digital gene expression data. Bioinformatics. 2010;26(1):139-40.
46. Kim A, Popovici J, Menard D, Serre D. Plasmodium vivax transcriptomes reveal stage-specific chloroquine response and differential regulation of male and female gametocytes. Nat Commun. 2019;10(1):371.
47. Mancio-Silva L, Gural N, Real E, Wadsworth MH, 2nd, Butty VL, March S, et al. A single-cell liver atlas of Plasmodium vivax infection. Cell Host Microbe. 2022;30(7):1048-60 e5.
48. Hoffman GE, Roussos P. Dream: powerful differential expression analysis for repeated measures designs. Bioinformatics. 2021;37(2):192-201.
49. Hoffman GE, Schadt EE. variancePartition: interpreting drivers of variation in complex gene expression studies. BMC Bioinformatics. 2016;17(1):483.
50. Gupta S, Singh S, Popovici J, Roesch C, Shakri AR, Guillotte-Blisnick M, et al. Targeting a Reticulocyte Binding Protein and Duffy Binding Protein to Inhibit Reticulocyte Invasion by Plasmodium vivax. Sci Rep. 2018;8(1):10511.
51. Hietanen J, Chim-Ong A, Chiramanewong T, Gruszczyk J, Roobsoong W, Tham WH, et al. Gene Models, Expression Repertoire, and Immune Response of Plasmodium vivax Reticulocyte Binding Proteins. Infect Immun. 2015;84(3):677-85.
52. Cui L, Miao J. Chromatin-mediated epigenetic regulation in the malaria parasite Plasmodium falciparum. Eukaryot Cell. 2010;9(8):1138-49.

53. Gupta AP, Chin WH, Zhu L, Mok S, Luah YH, Lim EH, et al. Dynamic epigenetic regulation of gene expression during the life cycle of malaria parasite Plasmodium falciparum. PLoS Pathog. 2013;9(2):e1003170.
54. Kepple D, Hubbard A, Ali MM, Abargero BR, Lopez K, Pestana K, et al. Plasmodium vivax From Duffy-Negative and Duffy-Positive Individuals Share Similar Gene Pools in East Africa. J Infect Dis. 2021;224(8):1422-31.
55. Ragotte RJ, Higgins MK, Draper SJ. The RH5-CyRPA-Ripr Complex as a Malaria Vaccine Target. Trends Parasitol. 2020;36(6):545-59.
56. Crosnier C, Bustamante LY, Bartholdson SJ, Bei AK, Theron M, Uchikawa M, et al. Basigin is a receptor essential for erythrocyte invasion by Plasmodium falciparum. Nature. 2011;480(7378):534-7.
57. Volz JC, Yap A, Sisquella X, Thompson JK, Lim NT, Whitehead LW, et al. Essential Role of the PfRh5/PfRipr/CyRPA Complex during Plasmodium falciparum Invasion of Erythrocytes. Cell Host Microbe. 2016;20(1):60-71.
58. Partey FD, Castberg FC, Sarbah EW, Silk SE, Awandare GA, Draper SJ, et al. Correction: Kinetics of antibody responses to PfRH5-complex antigens in Ghanaian children with Plasmodium falciparum malaria. PLoS One. 2018;13(9):e0204452.
59. Sierra AY, Barrero CA, Rodriguez R, Silva Y, Moncada C, Vanegas M, et al. Splenectomised and spleen intact Aotus monkeys' immune response to Plasmodium vivax MSP-1 protein fragments and their high activity binding peptides. Vaccine. 2003;21(27-30):4133-44.
60. Rougeron V, Elguero E, Arnathau C, Acuna Hidalgo B, Durand P, Houze S, et al. Human Plasmodium vivax diversity, population structure and evolutionary origin. PLoS Negl Trop Dis. 2020;14(3):e0008072.
61. Benavente ED, Manko E, Phelan J, Campos M, Nolder D, Fernandez D, et al. Distinctive genetic structure and selection patterns in Plasmodium vivax from South Asia and East Africa. Nat Commun. 2021;12(1):3160.
62. Bernabeu M, Lopez FJ, Ferrer M, Martin-Jaular L, Razaname A, Corradin G, et al. Functional analysis of Plasmodium vivax VIR proteins reveals different subcellular localizations and cytoadherence to the ICAM-1 endothelial receptor. Cell Microbiol. 2012;14(3):386-400.
63. Requena P, Rui E, Padilla N, Martinez-Espinosa FE, Castellanos ME, Botto-Menezes C, et al. Plasmodium vivax VIR Proteins Are Targets of Naturally-Acquired Antibody and T Cell Immune Responses to Malaria in Pregnant Women. PLoS Negl Trop Dis. 2016;10(10):e0005009.
64. Cook J, Speybroeck N, Sochanta T, Somony H, Sokny M, Claes F, et al. Sero-epidemiological evaluation of changes in Plasmodium falciparum and Plasmodium vivax transmission patterns over the rainy season in Cambodia. Malar J. 2012;11:86.
65. Kumar M, Skillman K, Duraisingh MT. Linking nutrient sensing and gene expression in Plasmodium falciparum blood-stage parasites. Mol Microbiol. 2021;115(5):891-900.
66. Alexandre MA, Benzecry SG, Siqueira AM, Vitor-Silva S, Melo GC, Monteiro WM, et al. The association between nutritional status and malaria in children from a rural community in the Amazonian region: a longitudinal study. PLoS Negl Trop Dis. 2015;9(4):e0003743.
67. McCurley AT, Callard GV. Characterization of housekeeping genes in zebrafish: male-female differences and effects of tissue type, developmental stage and chemical treatment. BMC Mol Biol. 2008;9:102.

68. Hollin T, Le Roch KG. From Genes to Transcripts, a Tightly Regulated Journey in Plasmodium. Front Cell Infect Microbiol. 2020;10:618454.
69. Hoo R, Zhu L, Amaladoss A, Mok S, Natalang O, Lapp SA, et al. Integrated analysis of the Plasmodium species transcriptome. EBioMedicine. 2016;7:255-66.
70. Liu F, Yang F, Wang Y, Hong M, Zheng W, Min H, et al. A conserved malaria parasite antigen Pb22 plays a critical role in male gametogenesis in Plasmodium berghei. Cell Microbiol. 2021;23(3):e13294.
71. Yuda M, Kaneko I, Murata Y, Iwanaga S, Nishi T. Mechanisms of triggering malaria gametocytogenesis by AP2-G. Parasitol Int. 2021;84:102403.
72. Abdelraheem MH, Bansal D, Idris MA, Mukhtar MM, Hamid MMA, Imam ZS, et al. Genetic diversity and transmissibility of imported Plasmodium vivax in Qatar and three countries of origin. Sci Rep. 2018;8(1):8870.
73. Bousema T, Okell L, Felger I, Drakeley C. Asymptomatic malaria infections: detectability, transmissibility and public health relevance. Nat Rev Microbiol. 2014;12(12):833-40.
74. Hofmann NE, Gruenberg M, Nate E, Ura A, Rodriguez-Rodriguez D, Salib M, et al. Assessment of ultra-sensitive malaria diagnosis versus standard molecular diagnostics for malaria elimination: an in-depth molecular community cross-sectional study. Lancet Infect Dis. 2018;18(10):1108-16.
75. Kosasih A, Koepfli C, Dahlan MS, Hawley WA, Baird JK, Mueller I, et al. Gametocyte carriage of Plasmodium falciparum (pfs25) and Plasmodium vivax (pvs25) during mass screening and treatment in West Timor, Indonesia: a longitudinal prospective study. Malar J. 2021;20(1):177.

Figures

Figure 1. (A) CIBERSORTx deconvolution of the 10 Ethiopian, four Cambodian, and two Brazilian *P. vivax* transcriptomes using a *P. berghei* homologue matrix. No significant difference was observed in the proportion of trophozoites and schizonts amongst the isolates ($p>0.05$). (B) Parasite stage based on microscopic analysis of five Ethiopian *P. vivax* samples. No significant difference was observed between microscopy and computational deconvolution for these samples ($p>0.05$).

Figure 2. Categorization of (A) all detectable transcripts and (B) upregulated (TPM > 20) transcripts for the Ethiopian *P. vivax* by gene function. The numbers shown represent the number of transcripts along with the overall percentage compared to all detected transcripts.

682 Transcripts that were not detected were removed from the analysis. Only transcripts involved
683 in transport and housekeeping showed a slight increase of 2.9% and 1.48%, respectively in
684 the number of upregulated transcripts, indicating a higher activity relative to the other
685 categories. By contrast, transcripts involved in RNA regulation, PIR, and ribosomal activity
686 showed a slight decrease of 2.19%, 1.79%, and 1.71%, indicating an overall lower activity
687 compared to other categories.

688 **Figure 3.** Heat map showing the top 30 highly transcribed genes based on *log*(2)CPM+1.
689 Genes are arranged by different functions as indicated on the y-axis. Overall, four genes
690 including PVP01_1000200 (PIR protein), PVP01_0202900 (18s rRNA), PVP01_0319600
691 (RNA-binding protein), and PVP01_0319500 (unknown function) from four different
692 functional groups were shown to be most highly expressed among the others. Of interest,
693 PVP01_0715400 (merozoite organizing protein), PVP01_0816800 (protein RIPR),
694 PVP01_1402400 (reticulocyte binding protein 2a), and PVP01_1469400 (reticulocyte
695 binding protein 3) were among the top 30 highly expressed genes involved in host
696 interactions.

697 **Figure 4.** (A) Comparisons of the entire transcriptomes with genes sorted by functionality
698 among the Ethiopian, Cambodian, and Brazilian *P. vivax*. The overall gene expression profile
699 was nearly identical between the Ethiopian and Cambodian *P. vivax*, but different from the
700 Brazilian isolates. Several genes involved in DNA regulation, host-interactions, replication,
701 ribosomal, and transportation were upregulated in the Ethiopian and Cambodian isolates but
702 showed considerable downregulation in Brazilian ones. (B-D) Volcano plots based on the
703 Kenward-Roger DE analyses comparing differentially expressed genes between the (B)
704 Ethiopian and Cambodian; (C) Ethiopian and Brazilian; (D) Cambodian and Brazilian

isolates. Blue dots represent single genes that are downregulated in the comparison while red dots represent upregulated genes by comparison. About 10% of the detectable transcripts were differentially expressed between the Ethiopian and Cambodian *P. vivax*, but about 25% and 27% variations were detected between the Ethiopian and Brazilian as well as the Cambodian and Brazilian *P. vivax*, respectively. Overall, the Brazilian isolates had more genes that were upregulated compared to the Ethiopian and Cambodian ones.

Figure 5. Heatmap showing 43 genes associated with erythrocyte binding function in the Ethiopian *P. vivax* based on *log*(2)TPM+1 values. *PvRBP*2b showed four-fold higher expression on average than *PvEBP/DBP*2, but 50% less than *PvDBP*1. *PvRBP*2a showed consistently the highest expression across all samples, with about 6-fold, 67-fold, and 15-fold higher expression than *PvDBP*1*, PvEBP/DBP*2, and *PvRBP*2b, respectively. Other genes including *PvMSP*3.8, *PvTRAg*14, and *PvTRAg*22 also showed higher expression than *PvDBP*1.

Figure 6. Comparisons of 43 genes associated with erythrocyte binding function based on *log*(2)TPM+1 values across the Ethiopian, Cambodian, and Brazilian *P. vivax* for (A) *PvDBP*1, *PvEBP*, and *PvRBP* genes; (B) *PvMSP* genes; (C) *PvTRAg* genes; (D) other putatively functional ligands. * denotes *P*-value < 0.05; ** denote *P*-value <0.01.

Figure 7. Heatmap comparing 26 *P. vivax* gametocyte biomarker candidates across the Ethiopian, Cambodian, and Brazilian *P. vivax*. Based on the expression level of *Pvs25*, all 10 *in vitro P. vivax* samples from Ethiopia, four samples from Cambodia, and two samples from Brazil contained gametocytes. Three genes, PVP01_1440800 (*PvAP2-G*), PVP01_1403000 (gametocyte associated protein, GAP), and PVP01_1208000 (*Pvs47*) from female and male

727 gametocytes, respectively, showed the highest expression across all geographical isolates,
728 and were consistently higher than *Pvs25*.
729
730 **Supplementary Files**
731 **Supplementary Table 1.** Name and gene ID of 43 candidate invasion genes.
732 **Supplementary Table 2.** Raw reads of 10 Ethiopian *P. vivax* transcriptomes in CPM and
733 TPM metrics, Raw reads of four Cambodian *P. vivax* transcriptomes in TPM metric, and
734 Raw reads of four Brazilian *P. vivax* transcriptomes in TPM metric.
735 **Supplementary Table 3.** Kenward-Roger DE analyses comparing the differentially
736 expressed genes between (a) Ethiopian and Cambodian, (b) Ethiopian and Brazilian, and (c)
737 Cambodian and Brazilian *P. vivax*.
738

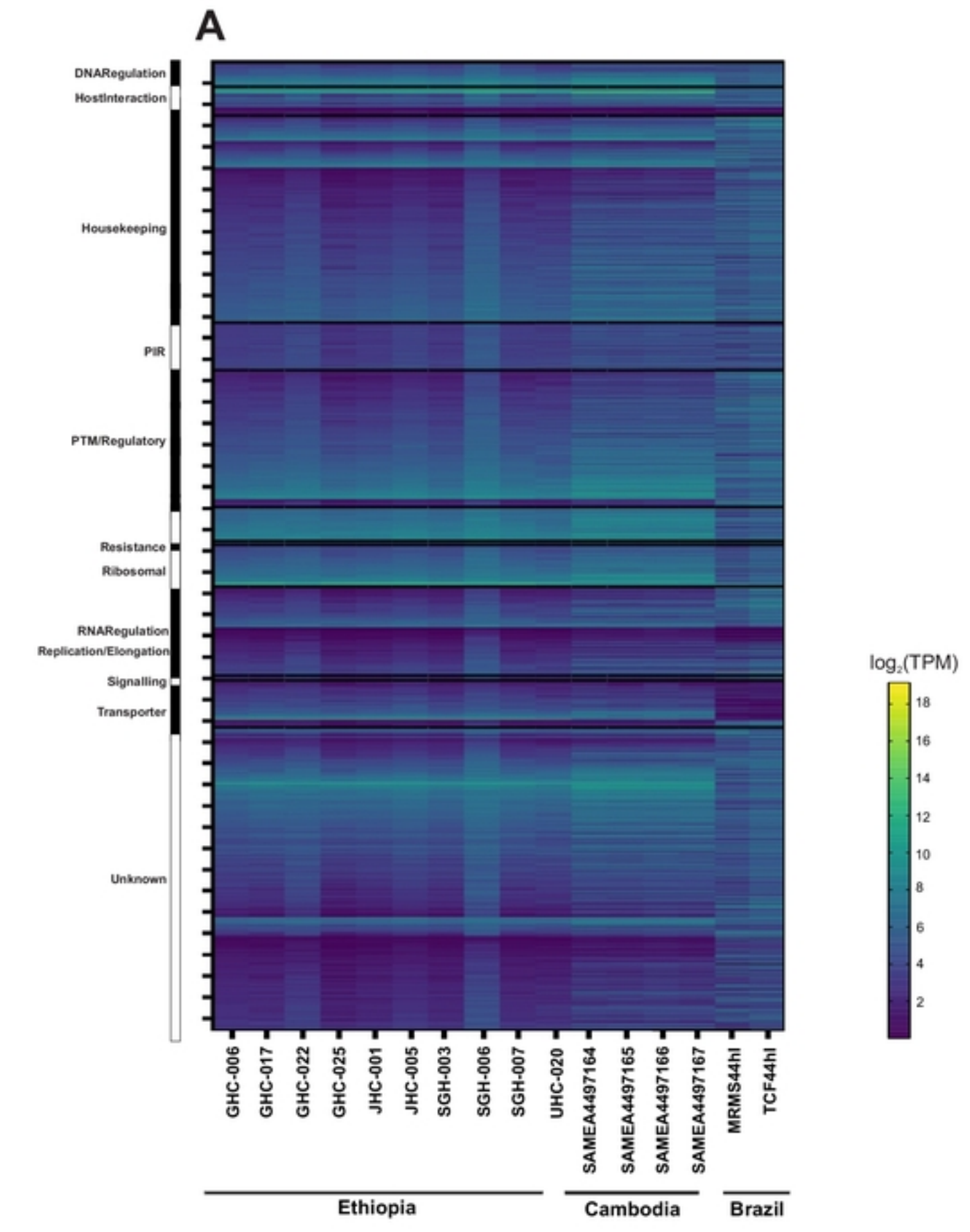

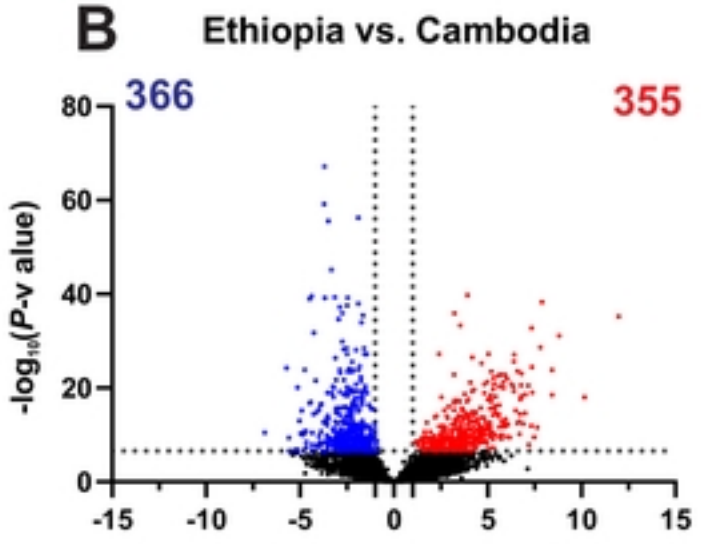

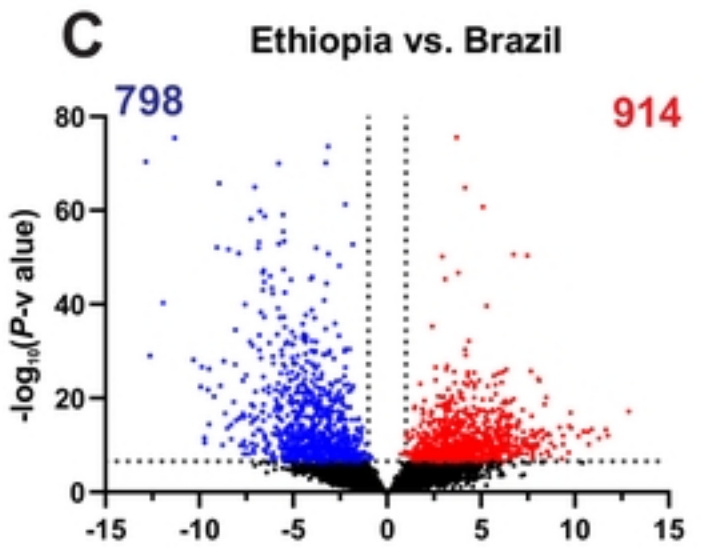

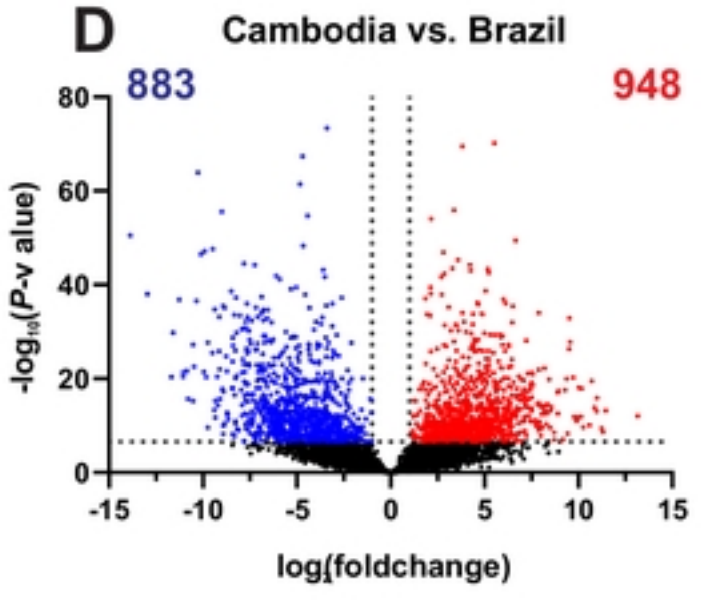

Figure 4

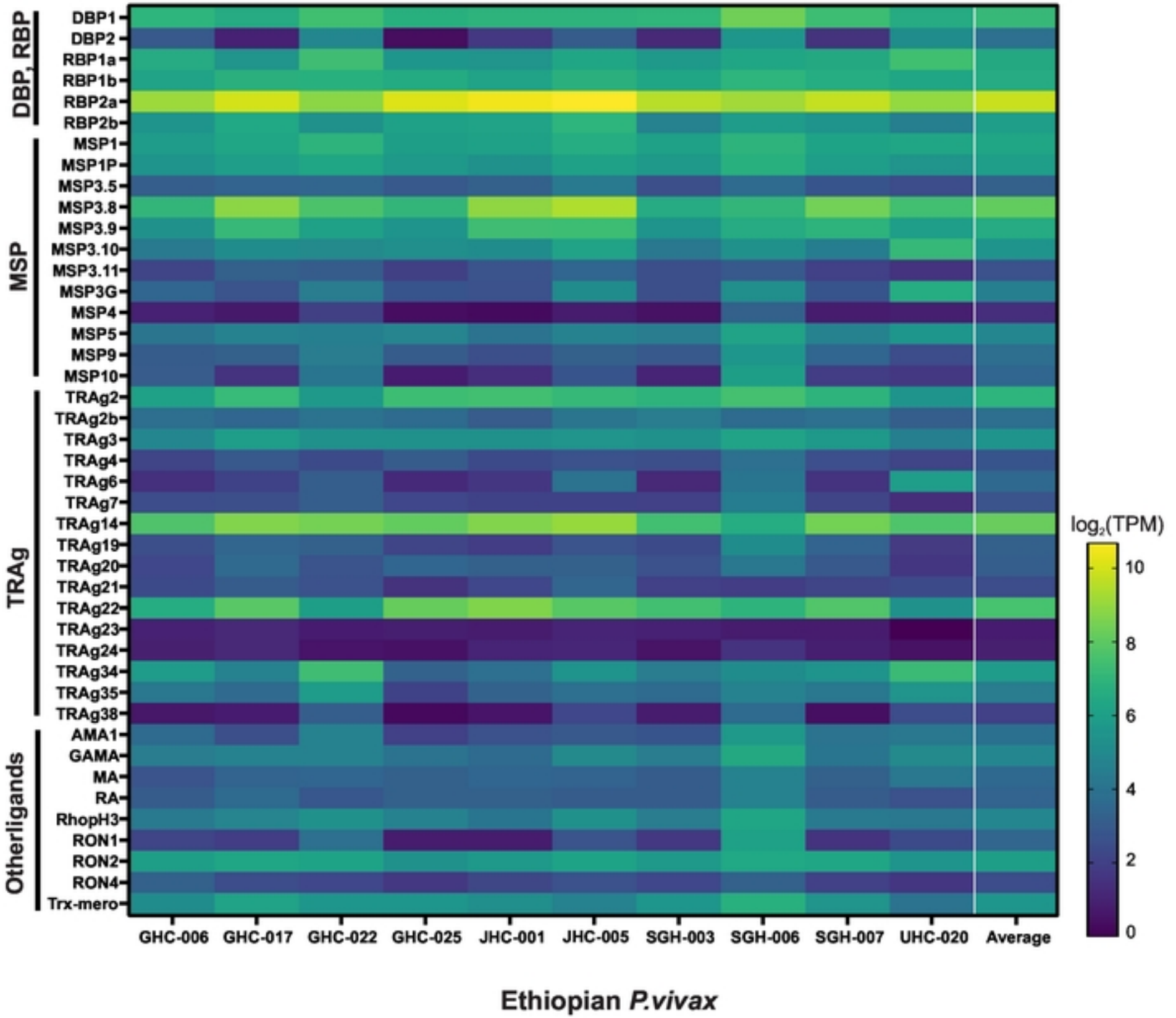
DBP, RBP
DBP1
DBP2
RBP1a
RBP1b
RBP2a
RBP2b
MSP
MSP1
MSP1P
MSP3.5
MSP3.8
MSP3.9
MSP3.10
MSP3.11
MSP3G
MSP4
MSP5
MSP9
MSP10
TRAg
TRAg2
TRAg2b
TRAg3
TRAg4
TRAg6
TRAg7
TRAg14
TRAg19
TRAg20
TRAg21
TRAg22
TRAg23
TRAg24
TRAg34
TRAg35
TRAg38
Otherligands
AMA1
GAMA
MA
RA
RhopH3
RON1
RON2
RON4
Trx-mero
GHC-006
GHC-017
GHC-022
GHC-025
JHC-001
JHC-005
SGH-003
SGH-006
SGH-007
UHC-020
Average
log2(TPM)
10
8
6
4
2
0
Ethiopian P.vivax

Figure 5

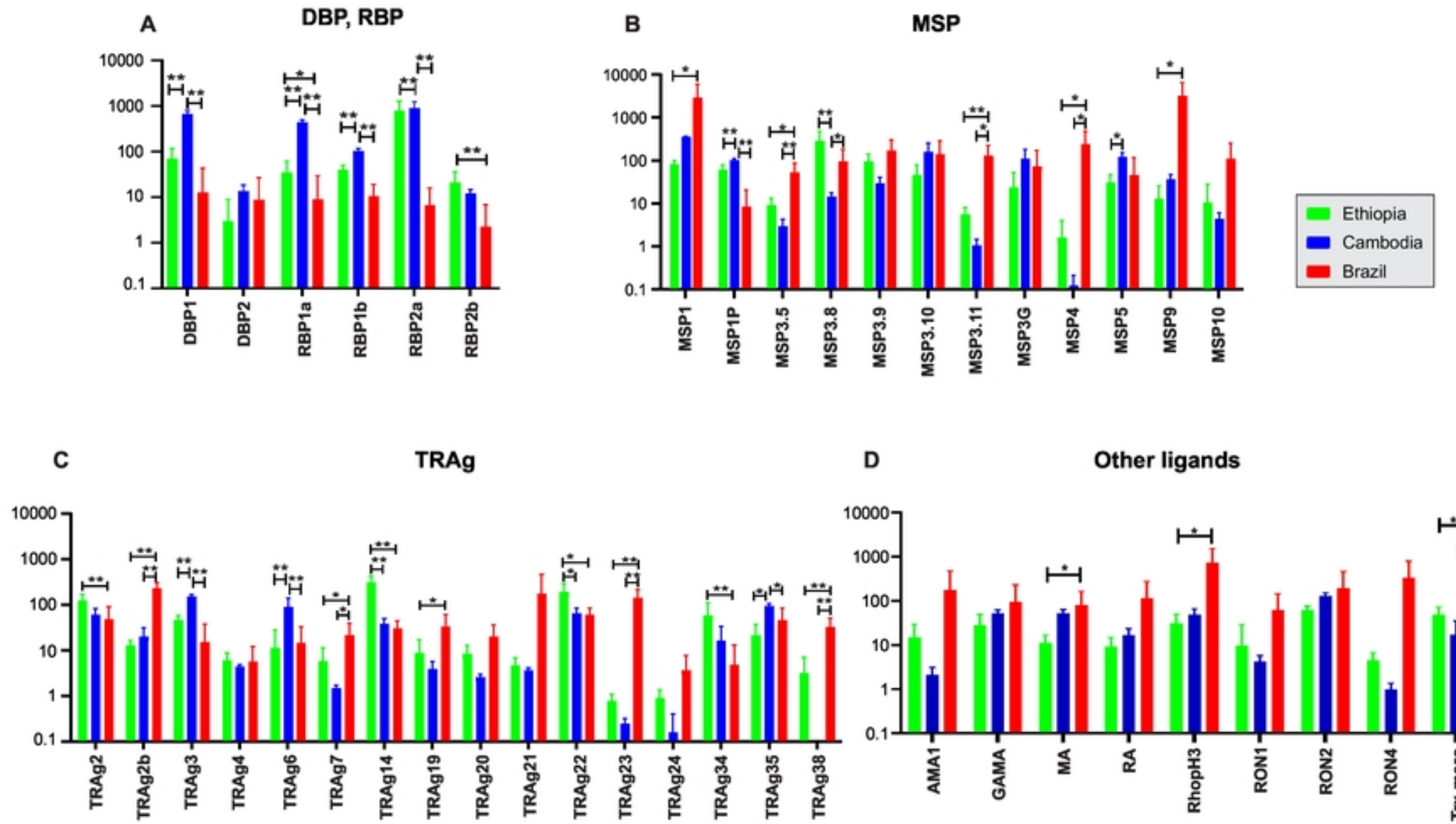
A
DBP, RBP
10000
1000
100
10
1
0.1
DBP1
DBP2
RBP1a
RBP1b
RBP2a
RBP2b
B
MSP
MSP1
MSP1P
MSP3.5
MSP3.8
MSP3.9
MSP3.10
MSP3.11
MSP3G
MSP4
MSP5
MSP9
MSP10
Ethiopia
Cambodia
Brazil
C
TRAg
TRAg2
TRAg2b
TRAg3
TRAg4
TRAg6
TRAg7
TRAg14
TRAg19
TRAg20
TRAg21
TRAg22
TRAg23
TRAg24
TRAg34
TRAg35
TRAg38
D
Other ligands
AMA1
GAMA
MA
RA
RhopH3
RON1
RON2
RON4
Trx-mero

Figure 6

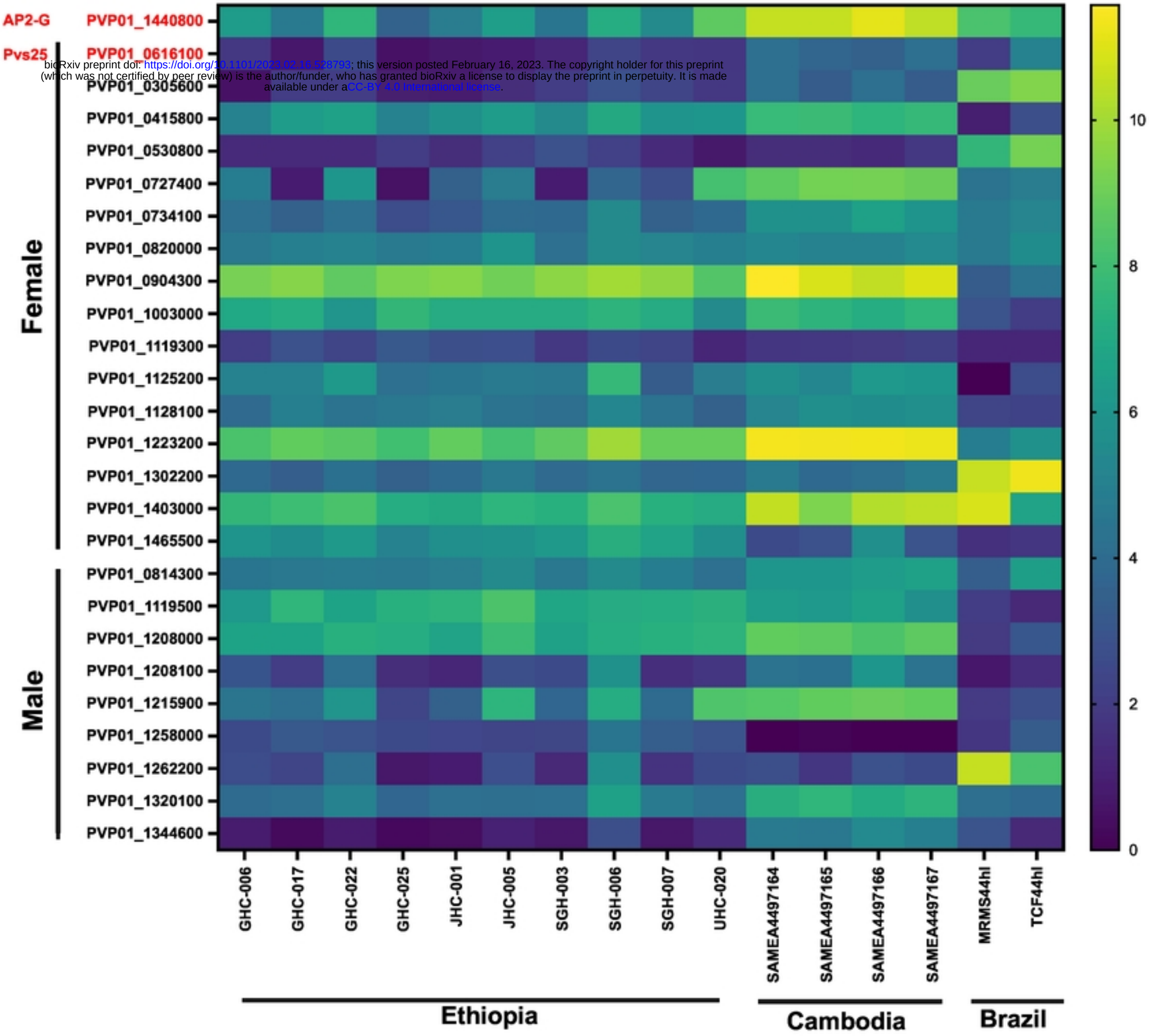

Figure 7

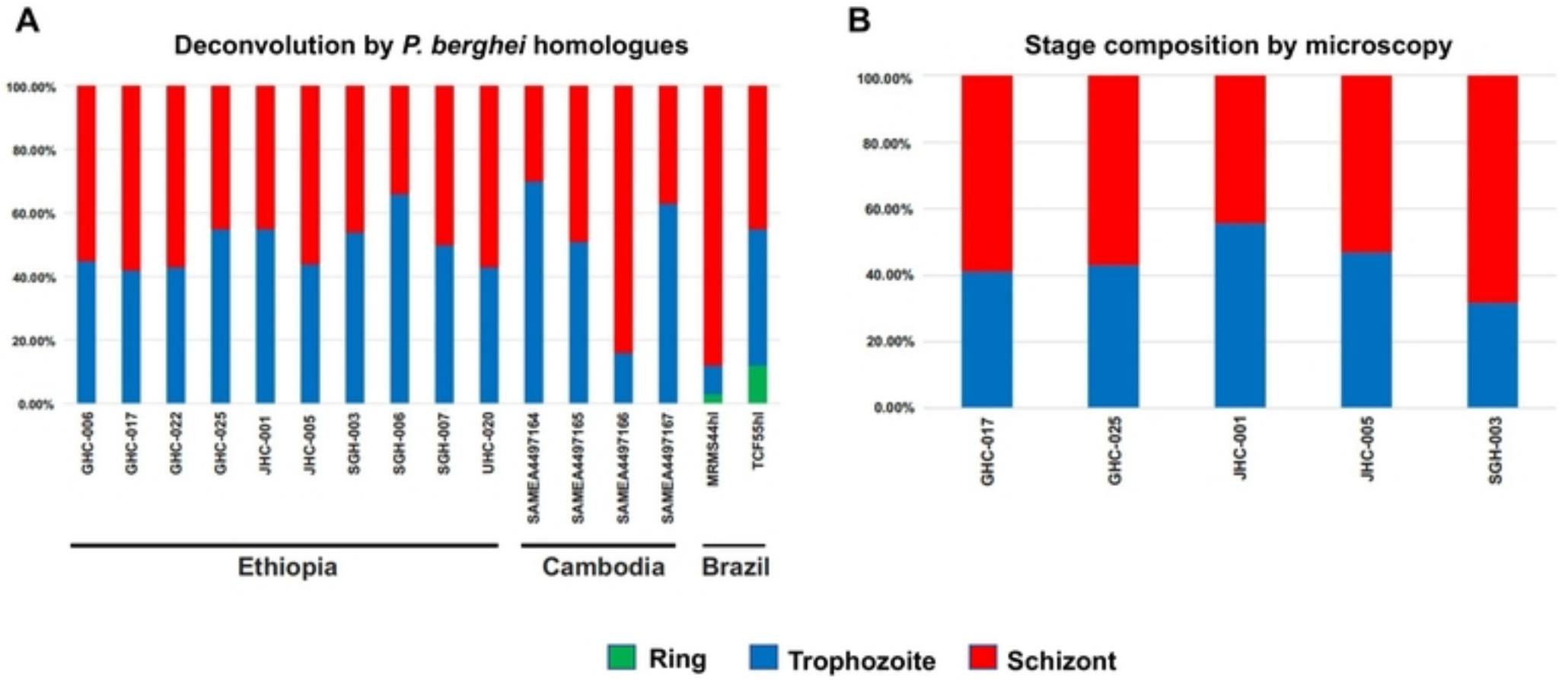
A
Deconvolution by P. berghei homologues
100.00%
80.00%
60.00%
40.00%
20.00%
0.00%
GHC-006
GHC-017
GHC-022
GHC-025
JHC-001
JHC-005
SGH-003
SGH-006
SGH-007
UHC-020
SAMEA4497164
SAMEA4497165
SAMEA4497166
SAMEA4497167
MRMS44hl
TCF55hl
Ethiopia
Cambodia
Brazil
B
Stage composition by microscopy
100.00%
80.00%
60.00%
40.00%
20.00%
0.00%
GHC-017
GHC-025
JHC-001
JHC-005
SGH-003
Ring
Trophozoite
Schizont

Figure 1

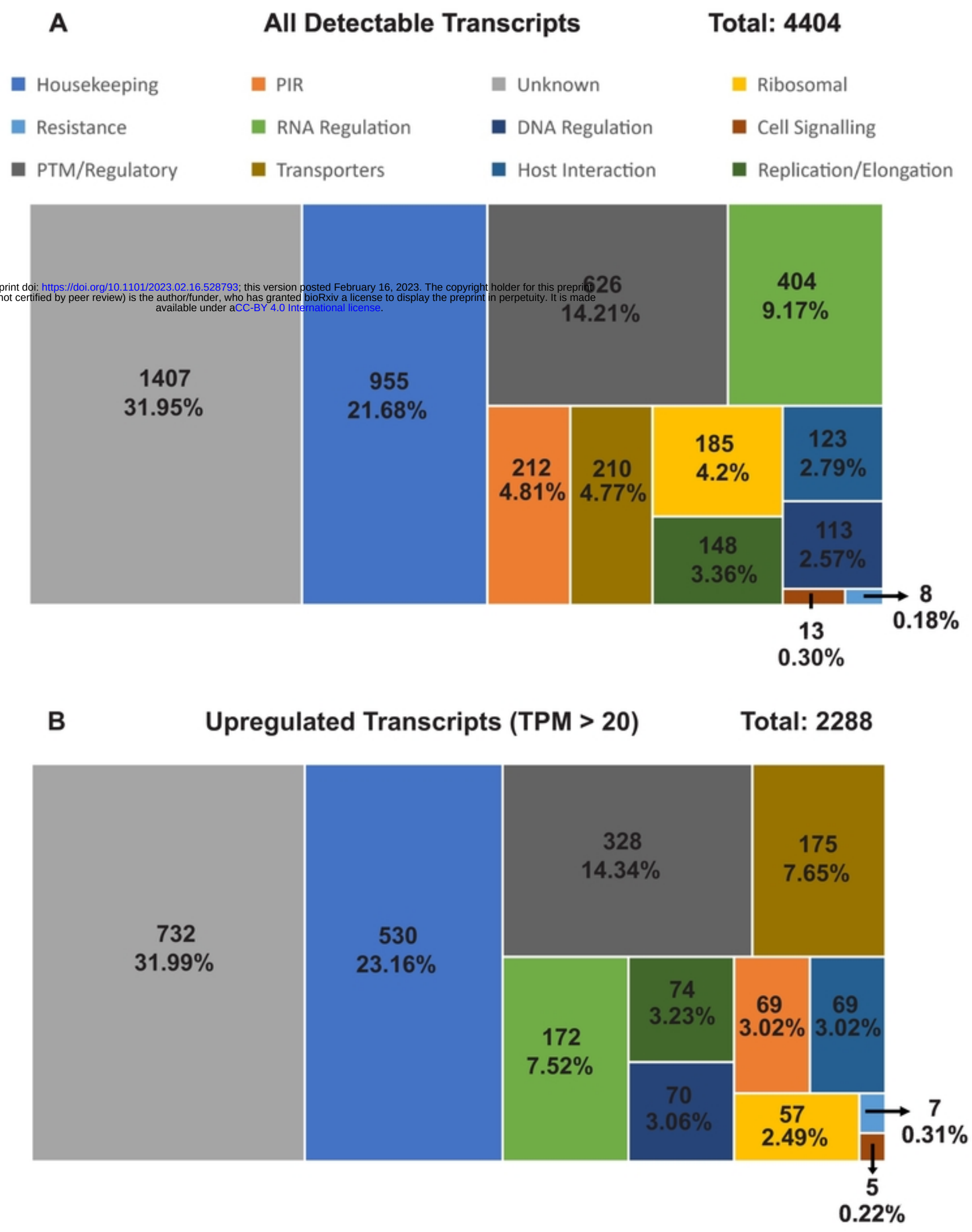

Figure 2

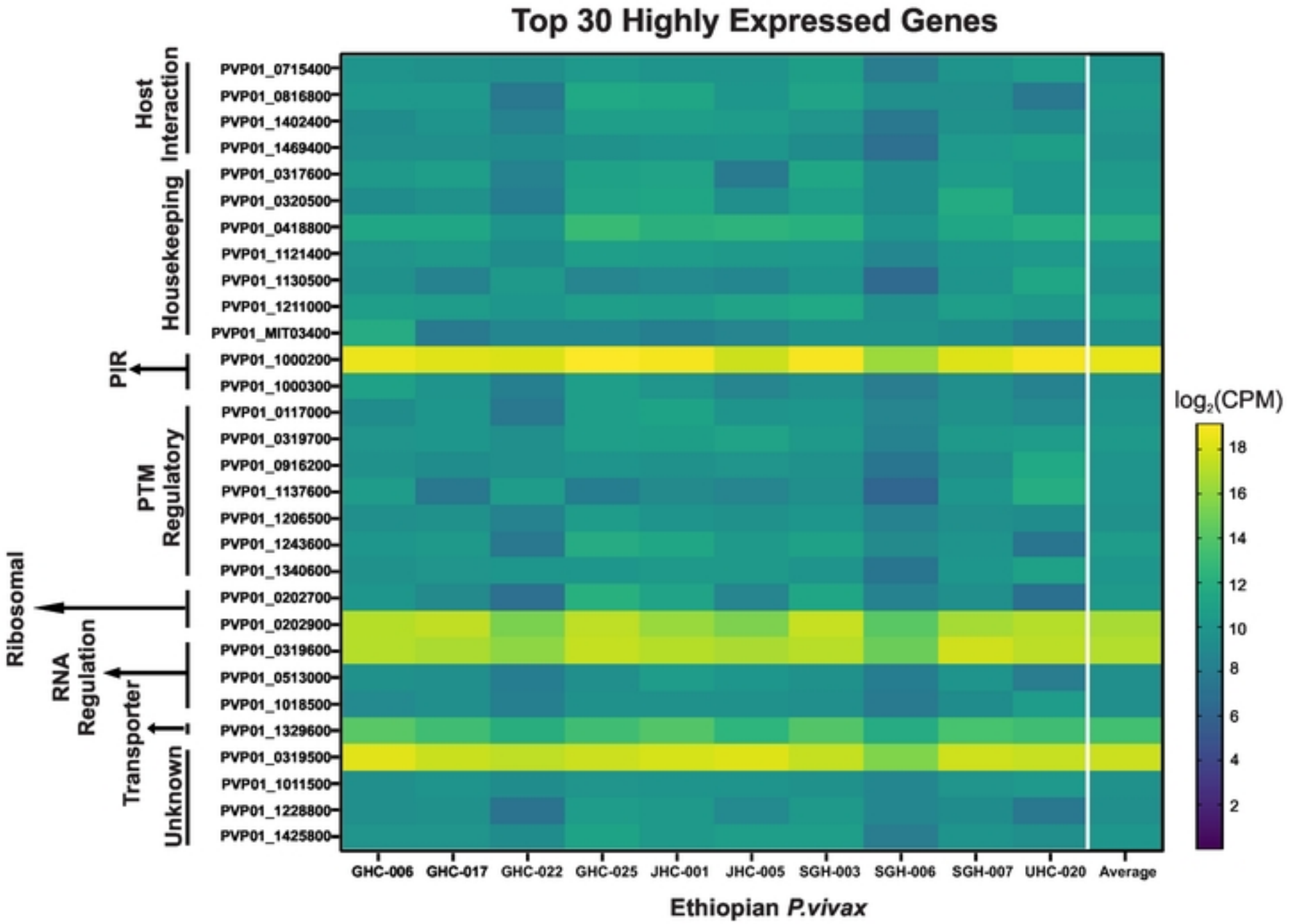
Top 30 Highly Expressed Genes
Host Interaction
Housekeeping
PIR
PTM Regulatory
Ribosomal
RNA Regulation
Transporter
Unknown
PVP01_0715400
PVP01_0816800
PVP01_1402400
PVP01_1469400
PVP01_0317600
PVP01_0320500
PVP01_0418800
PVP01_1121400
PVP01_1130500
PVP01_1211000
PVP01_MIT03400
PVP01_1000200
PVP01_1000300
PVP01_0117000
PVP01_0319700
PVP01_0916200
PVP01_1137600
PVP01_1206500
PVP01_1243600
PVP01_1340600
PVP01_0202700
PVP01_0202900
PVP01_0319600
PVP01_0513000
PVP01_1018500
PVP01_1329600
PVP01_0319500
PVP01_1011500
PVP01_1228800
PVP01_1425800
GHC-006
GHC-017
GHC-022
GHC-025
JHC-001
JHC-005
SGH-003
SGH-006
SGH-007
UHC-020
Average
Ethiopian P.vivax
log2(CPM)
18
16
14
12
10
8
6
4
2

Figure 3